DISCIPLINARUM SCIENTIA *Disciplinarum Scientia.* **Série: Naturais e Tecnológicas**
Santa Maria, v. 25, n. 2, p. 257-272, 2024
Recebido em: 26.07.2024. Aprovado em: 19.09.2024.
ISSN 2176-462X | DOI: doi.org/10.37779/nt.v25i2.5035

ENHANCED DEGRADATION OF CRYSTAL VIOLET DYE USING MULTI-PHASE DOPED ZrO_2 AND HfO_2 CATALYSTS

DEGRADAÇÃO APRIMORADA DO CORANTE CRISTAL VIOLETA USANDO CATALISADORES DE ZrO_2 E HfO_2 DOPADOS EM MÚLTIPLAS FASES

Giovanni Miraveti Carriello[1], Guilherme Manassés Pegoraro[2], Lucas Repecka Alves[3], Amanda Stefanie Jabur de Assis[4], Juliana Cristina Ramos de Oliveira[5], Gabriela Santos[6], Iolanda Cristina Silveira Duarte[7], Aparecido Junior de Menezes[8] e Giovanni Pimenta Mambrini[9]

ABSTRACT

The study investigated the efficiency of zirconium oxide (ZrO_2) and hafnium oxide (HfO_2) based materials doped with Ag and Pr in the degradation of the dye crystal violet, a mutagenic and carcinogenic compound widely used in industrial processes. Due to their high solubility in water, synthetic dyes represent a challenge for removal by conventional methods, requiring more effective approaches. The research revealed that the presence of multiple phases in the studied materials significantly increases the efficiency in dye degradation, with values ranging between 66% ± 3 and 71% ± 5, suggesting that the diversity of phases provides a greater variety of active catalytic sites. In contrast, single-phase materials, such as ZrO_2 and HfO_2 stabilized in cubic and monoclinic phases, respectively, showed lower degradation rates, all below 37% ± 11.

Keywords: photocatalysis; synthetic dyes; water pollution.

RESUMO

O estudo investigou a eficiência de materiais baseados em óxido de zircônio (ZrO_2) e óxido de háfnio (HfO_2) dopados com Ag e Pr na degradação do corante cristal violeta, um composto mutagênico e carcinogênico amplamente utilizado em processos industriais. Devido à sua alta solubilidade em água, corantes sintéticos representam um desafio para remoção por métodos convencionais, exigindo abordagens mais eficazes.

1 PhD student in the Graduate Program in Materials Science (PPGCM) at the Federal University of São Carlos (UFSCar). E-mail: giovannimiraveti@estudante.ufscar.br. ORCID: https://orcid.org/0000-0003-2725-0328

2 PhD student in the Graduate Program in Materials Science (PPGCM) at the Federal University of São Carlos (UFSCar). E-mail: guilherme.pegoraro@estudante.ufscar.br. ORCID: https://orcid.org/0000-0001-9075-7952

3 PhD student in the Graduate Program in Materials Science (PPGCM) at the Federal University of São Carlos (UFSCar). E-mail: lucasrepecka@estudante.ufscar.br. ORCID: https://orcid.org/0000-0001-5458-2403

4 PhD student in the Graduate Program in Biotechnology and Environmental Monitoring (PPGBMA) at the Federal University of São Carlos (UFSCar). E-mail: amanda.jabur@gmail.com. ORCID: https://orcid.org/0000-0002-2675-2898

5 PhD student in the Graduate Program in Biotechnology and Environmental Monitoring (PPGBMA) at the Federal University of São Carlos (UFSCar). E-mail: julianac_ramos@yahoo.com.br. ORCID: https://orcid.org/0000-0002-9378-0880

6 Undergraduate student in Biological Sciences at the Federal University of São Carlos (UFSCar). E-mail: gabriela.santos@estudante.ufscar.br. ORCID: https://orcid.org/0009-0009-0851-574X

7 Professor at the Federal University of São Carlos (UFSCar), Department of Biology (DBio). E-mail: iolanda@ufscar.br. ORCID: https://orcid.org/0000-0002-9141-1010

8 Professor at the Federal University of São Carlos (UFSCar), Department of Physics, Chemistry, and Mathematics (DFQM). E-mail: jrmenezes@ufscar.br. ORCID: https://orcid.org/0000-0001-5638-489X

9 Professor at the Federal University of São Carlos (UFSCar), Department of Physics, Chemistry, and Mathematics (DFQM). E-mail: gpmambrini@ufscar.br. ORCID: https://orcid.org/0000-0001-8943-5876

A pesquisa revelou que a presença de múltiplas fases nos materiais estudados aumenta significativamente a eficiência na degradação do corante, com valores entre 66% ± 3 e 71% ± 5, sugerindo que a diversidade de fases proporciona uma maior variedade de sítios catalíticos ativos. Em contrapartida, materiais com uma única fase, como ZrO_2 e HfO_2 estabilizados em fases cúbica e monoclínica, respectivamente, apresentaram menores taxas de degradação, todas abaixo de 37% ± 11.

Palavras-chave: *fotocatálise; corantes sintéticos; poluição hídrica.*

INTRODUCTION

The deposition of synthetic dyes in the environment, especially through wastewater from the textile, paper and leather industries, hospitals, universities, food and pharmaceutical industries, represents a significant challenge due to their harmful effects, even at low concentrations (ARDILA-LEAL *et al.*, 2021). During the dyeing process, approximately 10-20% of dyes are discarded into the environment, further aggravating contamination (KUMARI *et al.*, 2023). Dyes, as they are soluble organic compounds, are difficult to remove from wastewater using conventional procedures due to their high solubility in water (SHINDHAL *et al.*, 2021). Among the most problematic dyes is crystal violet, known for its mutagenic and carcinogenic nature, persistence and ability to infiltrate groundwater, making it a significant pollutant (FAIZAN; BAKHTAWARA; ALI SHAH, 2022; SINGH; TOMAR; SINGH, 2024). It is one of the dyes used in the dyeing of polymers, such as nylon and wool, and since about 12% of synthetic dyes are released during the dyeing process, it becomes crucial to investigate methods for treating this type of waste (MANI; BHARAGAVA, 2016).

The efficiency of dye removal techniques is therefore of great importance to the scientific community. Several techniques, including chemical oxidation, electrochemical treatment, coagulation, biological treatment, photocatalytic degradation and adsorption, have demonstrated effectiveness in treating wastewater contaminated with crystal violet (SINGH; TOMAR; SINGH, 2024). Research with this focus is important when considering Goals 6 and 14 of the Sustainable Development Goals, which address the sustainable management of water and sanitation for all, and the conservation and use of aquatic resources (KHOSLA *et al.*, 2021). In this context, materials such as zirconium dioxide (ZrO_2) and hafnium dioxide (HfO_2) have gained prominence due to their unique properties and high thermal and chemical stability.

The polymorphism and catalytic action of ZrO_2 and HfO_2 are topics of considerable importance in materials science due to their wide technological applications. Both materials have multiple crystalline forms that can be induced and stabilized by external factors, such as temperature, pressure and doping, directly influencing their physical, chemical and mechanical properties. ZrO_2, for example, exhibits attractive physical, mechanical and electrical properties as well as high chemical durability, making it suitable for diverse technological applications such as thermal barrier coatings, gas and electrolyte sensors in solid oxide fuel cells (LU *et al.*, 2011). In relation to its band gap, when it is in the monoclinic phase, it has an approximate value of 5.8 eV (LI *et al.*, 2017), nd in the cubic phase, approximately 3.84 eV (ZANDIEHNADEM; MURRAY; CHING, 1988). Similarly, HfO_2 has several crystalline structures, with

the monoclinic phase being the most stable at room temperature (LAUDADIO *et al*., 2022). Doping can stabilize other polymorphic forms, such as the orthorhombic and cubic phases, crucial for ferroelectric behavior (PAVONI *et al*., 2022). In relation to its band gap, pure HfO_2 in the monoclinic phase is estimated to have a value around 5.83 eV, and the cubic phase, slightly higher, around 5.88 eV (ONDRAČKA *et al*., 2016).

Both materials play an important role in catalytic applications. ZrO_2, due to its unique surface properties and high thermal stability, is widely used as a catalyst support, where different crystalline phases provide distinct surface characteristics, such as oxygen vacancies and basic hydroxyl groups (HU *et al*., 2020). On the other hand, HfO_2, with a greater electron density in its oxygen atoms compared to ZrO_2, presents advantages for photocatalytic applications, especially in the UV region, due to its ability to capture photogenerated electrons (KOCYIGIT *et al*., 2024). Furthermore, Ag@ HfO_2 nanocomposites have shown high efficiency in the photodegradation of dyes, highlighting the potential of HfO_2 as a shell material to capture more charge carriers on the surface and optimize the photocatalytic degradation of pollutants (KOCYIGIT *et al*., 2024).

Doping ZrO_2 and HfO_2 with elements such as silver (Ag) and praseodymium (Pr) can further improve their catalytic and photocatalytic properties. Ag doping, for example, can increase the capture efficiency of photogenerated electrons (KOCYIGIT *et al*., 2024), while Pr doping can introduce intermediate electronic states that facilitate charge transfer and degradation of organic contaminants (DUDEK *et al*., 2011; LIANG *et al*., 2009). Thus, the combination of ZrO_2 and HfO2 doped with Ag and Pr presents a promising approach for the efficient removal of dyes such as crystal violet from wastewater.

The synergy between the high thermal and chemical stability properties of metal oxides and the increased efficiency provided by doping with metals and rare earths can result in highly effective catalytic materials for environmental applications, significantly contributing to the mitigation of environmental impacts caused by dye contamination (BALARAM, 2019; GIONCO *et al*., 2017) Ce, Pr, Nd, Pm, Sm, Eu, Gd, Tb, Dy, Ho, Er, Tm, Yb, and Lu. Understanding and controlling the polymorphisms and phase transformations of ZrO_2 and HfO_2 are, therefore, fundamental to optimizing their properties and expanding their technological applications, from advanced nuclear systems to catalysts and photocatalytic devices (LU *et al*., 2011; PAVONI *et al*., 2022). Therefore, the present study aims to study the efficiency of ZrO_2 and HfO_2 doped with Ag and Pr in the degradation of crystal violet dye and advance research and development of materials to solve critical environmental challenges.

METHODOLOGY

PRODUCTION

All samples were prepared following the methodology outlined by Ramos-González *et al.* (2010) for HfO_2, known as the polymeric precursors method. To achieve this, aqueous solutions

were prepared containing 0.0001 mol/L of metallic ions and 0.0003 mol/L of citric acid (99.5%, Synth, Brazil). The zirconium precursor used was $ZrOCl_2 \cdot_8 H2O$ (99.0%, ACS Científica, Brazil) and silver precursor was $AgNO_3$ (99.0%, Synth, Brazil). Hafnium and praseodymium were synthesized from the metallic elements. Metallic hafnium (99.95%, Chengshuo, China) was dissolved in H_2SO_4 (98%, Synth, Brazil), precipitated with ammonia hydroxide, and the resulting precipitate was dissolved in HCl (37%, Synth, Brazil) and then dried at room temperature to obtain crystals of $HfOCl_2 \cdot 8H_2O$ (CARRIELLO *et al.*, 2024). Metallic praseodymium (99.9%, Peguys, Israel) was dissolved in HCl and dried at room temperature to obtain crystals of $PrCl_3 \cdot 7H_2O$. Samples doped with 10% ± 1 received $AgNO_3$ and $PrCl_3 \cdot 7H_2O$ in the initial solution. The solution was heated to 90 °C, and ethylene glycol (QuimisulSC, Brazil) was added in a proportion of 4 mols of ethylene glycol to every mol of citric acid. The solution was evaporated to dryness, and the system was left in a heating oven for 12 hours at 120 °C. Subsequently, the samples were calcined at 500 °C for two hours, except for the hafnium sample doped with silver, which was calcined at 600 °C. The choice of praseodymium for doping was made because the literature indicates the stabilization of ZrO_2 and HfO_2 in the cubic structure (LIU *et al.*, 2019; RAMOS-BRITO *et al.*, 2004), nd silver doping due to research showing that $Ag@ZrO_2$ and $Ag@HfO_2$ nanocomposites are effective in treating pollutants in aqueous media (MAHAM; NASROLLAHZADEH; MOHAMMAD SAJADI, 2020; KOCYIGIT *et al.*, 2024).

CHARACTERIZATION

The samples were characterized using a Shimadzu XRD-6100 X-ray diffractometer, operating with a copper electrode at 40.0 kV and 30.0 mA. The analysis was conducted in the range from 5° to 80° with a scanning rate of 1.00 degree per minute. Additionally, the samples were examined using a benchtop scanning electron microscope (Hitachi TM3000) coupled with an energy-dispersive spectrometer. Dynamic light scattering was used to characterize each sample, using water as a solvent for dispersion, a measurement time of 10 s with a target temperature of 25 ºC and a maximum number of 30 runs on an Anton Paar Litesizer DLS 500 instrument with the Kalliope software.

PHOTOCATALYTIC ACTIVITY

The dye degradation assays, conducted in duplicate, took place in a UV chamber, as described by Vaz (2008), using UV-C lamps with a peak emission at 254 nm. The methodology was adapted from Liang (2009), employing 1% of the catalyst suspension in a solution of 0.001% commercial crystal violet prepared from a commercial crystal violet solution (1%, UNIPHAR, Brazil). The samples

were exposed to the UV chamber for 1 hour and quantified using a Thermo Scientific Genesys 10UV UV-visible spectrophotometer. The assays were performed in duplicate. A blank assay was also conducted, which consists of adding the crystal violet solution, without the catalyst, in the UV chamber.

RESULTS AND DISCUSSION

X-RAY DIFFRACTOMETRY

The diffractograms of the samples, along with the ICDD cards 13-307, 20-684, 2-733, and 1-1013, corresponding, respectively, to monoclinic ZrO_2, cubic ZrO_2, tetragonal ZrO_2, and cubic AgCl (chlorargyrite), are depicted in Figure 1.

Figure 1 - Sample Diffractograms and ICDD Cards: 13-307 (ZrO_2 monoclinic), 20-684 (ZrO_2 cubic), 2-733 (ZrO_2 tetragonal), and 1-1013 (AgCl chlorargyrite).

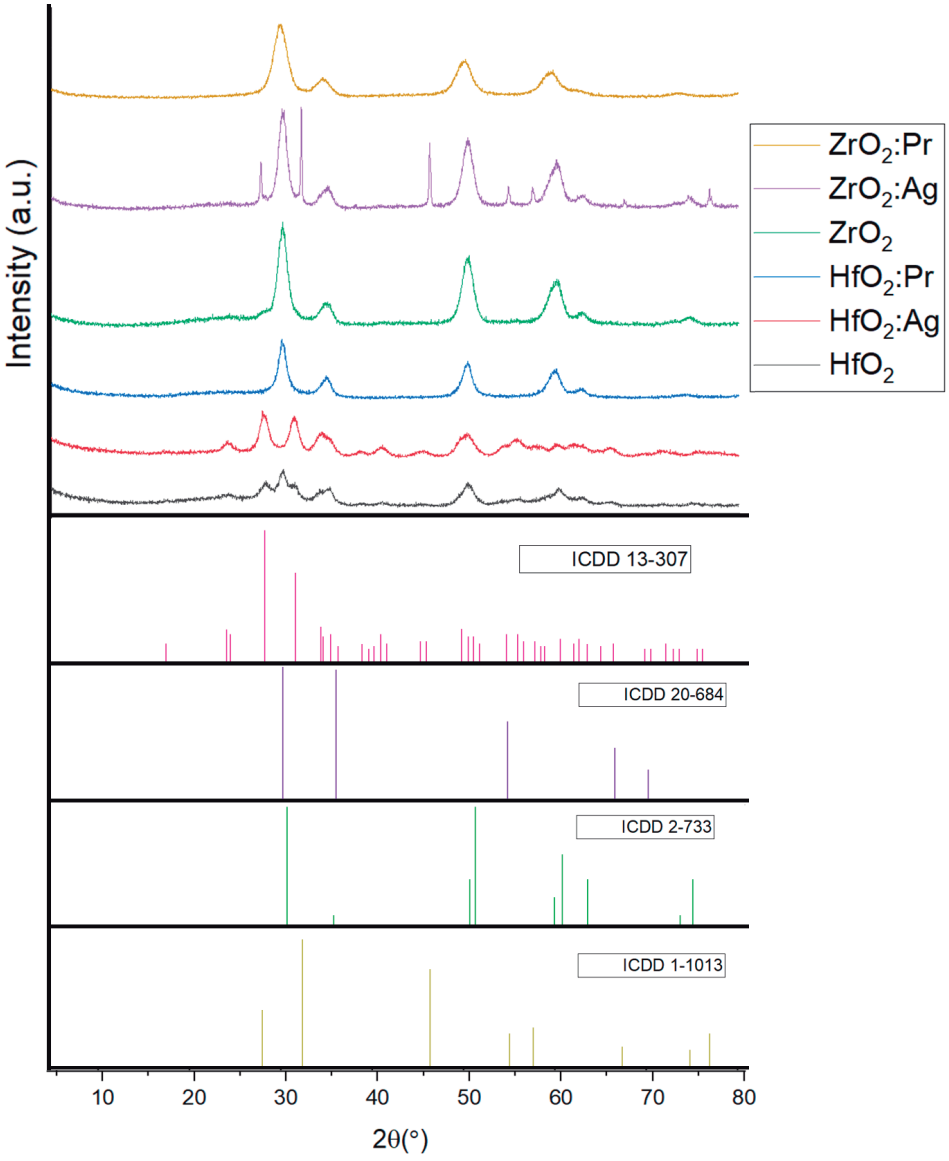

Source: Authors.

Given the similarities between zirconium and hafnium, their characterization cards are also similar. For instance, the ICCD card 53-550 for cubic HfO2 is akin to ICCD 20-684 for cubic ZrO_2, and ICCD 74-1506 for monoclinic HfO_2 resembles ICCD 13-307 for monoclinic ZrO_2. The HfO_2 sample exhibited two phases, monoclinic and cubic, as expected, as described by Ramos-González et al (2010). The ZrO_2 sample showed a tetragonal structure, consistent with previous literature reports for temperatures below 600 °C (NERIS *et al.*, 2020).

Stabilization in the cubic phase of ZrO_2 and HfO_2 with lanthanide ions has been extensively explored in the literature (LAURIA *et al.*, 2013; SAAD; MARTINEZ; TRICE, 2023; SALAVATI-NIASARI; DADKHAH; DAVAR, 2009). The attainment of the monoclinic phase of HfO_2 when doped with silver can be attributed to the temperature of 600 °C at which the sample was calcined (RAMOS-GONZÁLEZ *et al.*, 2010). The ZrO_2:Ag sample, on the other hand, appeared as a three-phase system, rich in tetragonal ZrO_2 and silver chloride, with small amounts of tetragonal ZrO_2. As seen in Figure 1, the most intense peaks of monoclinic ZrO_2 are close to silver chloride; however, upon magnifying the graph, they can be observed, as seen in Figure 2.

Figure 2 - Amplification of monoclinic ZrO_2 diffraction peaks in the presence of AgCl chlorargyrite.

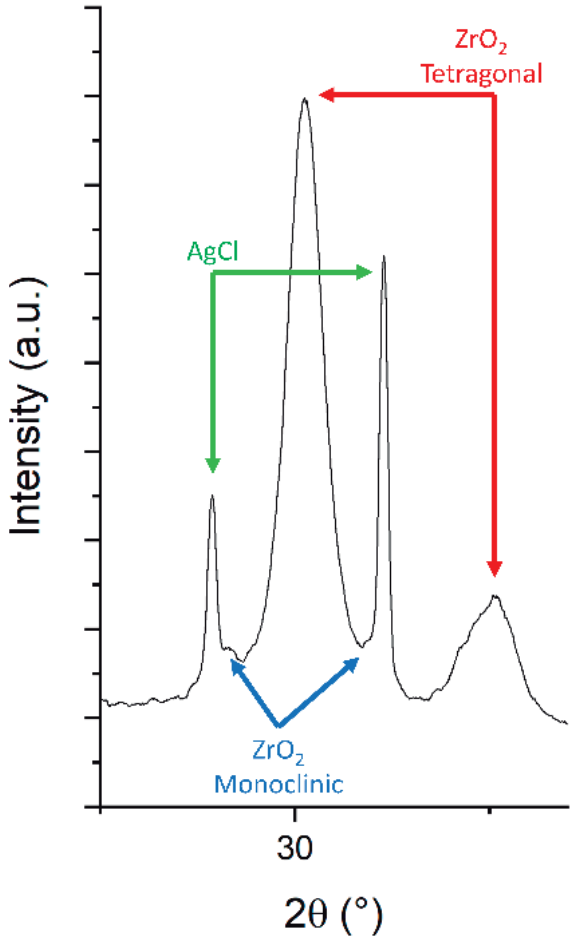

Source: Author's Construction.

Using the Scherrer equation, it is possible to estimate the average crystallite size for all the materials used (HARGREAVES, 2016). For this, the peak near 30° was selected for samples that contain cubic or tetragonal phases, and the peak near 29° for samples that showed the monoclinic phase. These values are shown in Table 1.

Table 1 - Average Crystallite Size Estimated from Peak Diffractions for Different Crystalline Phases

Sample	Average Crystallite Size (nm)
ZrO_2	8.07 ± 0.02 (tetragonal)
ZrO_2:Ag	68.0 ± 0.2 (monoclinic) 9.23 ± 0.02 (tetragonal)
ZrO_2:Pr	5.28 ± 0.02 (cubic)
HfO_2	3.41 ± 0.02 (monoclinic)
HfO_2:Ag	10,4 ± 0.02 (cubic) 7.37 ± 0.02 (monoclinic)
HfO_2:Pr	9.63 ± 0.02 (cubic)

Source: Author's Construction.

A variation in crystallite size is observed according to the material and the applied dopings. For example, pure ZrO_2 presents crystallites with an average size of 8.07 nm in the tetragonal phase, while doping with Ag results in larger crystallites, measuring 68.0 nm, in the monoclinic phase (less abundant in the sample, as seen in Figure 2, where the low intensity of the monoclinic peaks can be observed), and smaller ones, measuring 9.23 nm, in the tetragonal phase. In the case of HfO_2, the crystallites in the pure monoclinic phase are significantly smaller (3.41 nm) compared to those doped with Ag (multiphase, with monoclinic and cubic phases) or Pr (purely cubic)

SCANNING ELECTRON MICROSCOPY

The figures below show the SEM images for each of the samples, with the elemental distribution of relevant elements as obtained from the SEM-coupled energy dispersive spectrometer.

Figure 3 - SEM image and EDS elemental distribution for ZrO_2 (t), ZrO_2:Ag (m/t) and ZrO_2:Pr (c).

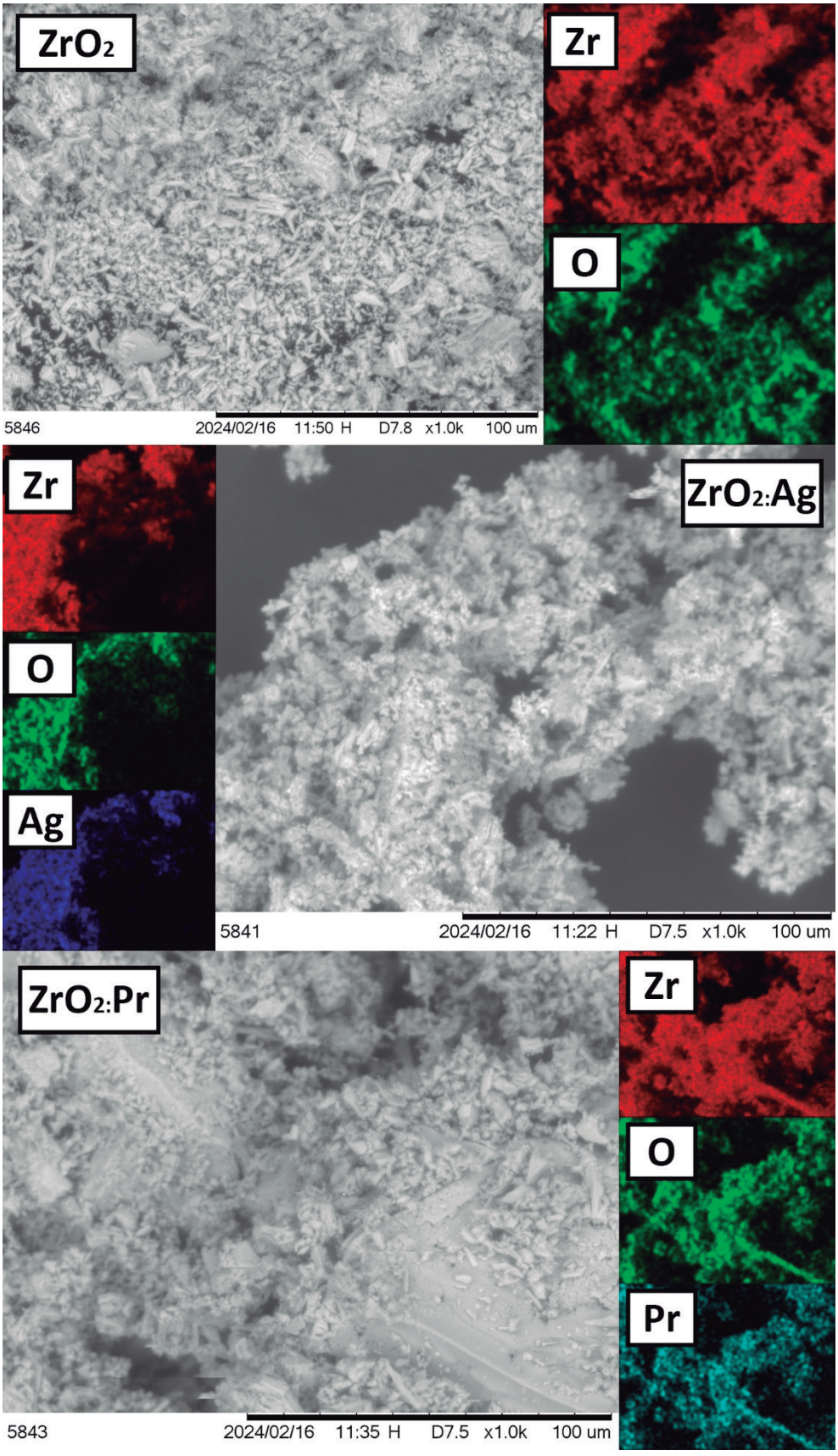

Source: Author's Construction.

Figure 4 - SEM image and EDS elemental distribution for HfO_2 (m/c), HfO_2:Ag (m) and HfO_2:Pr (c).

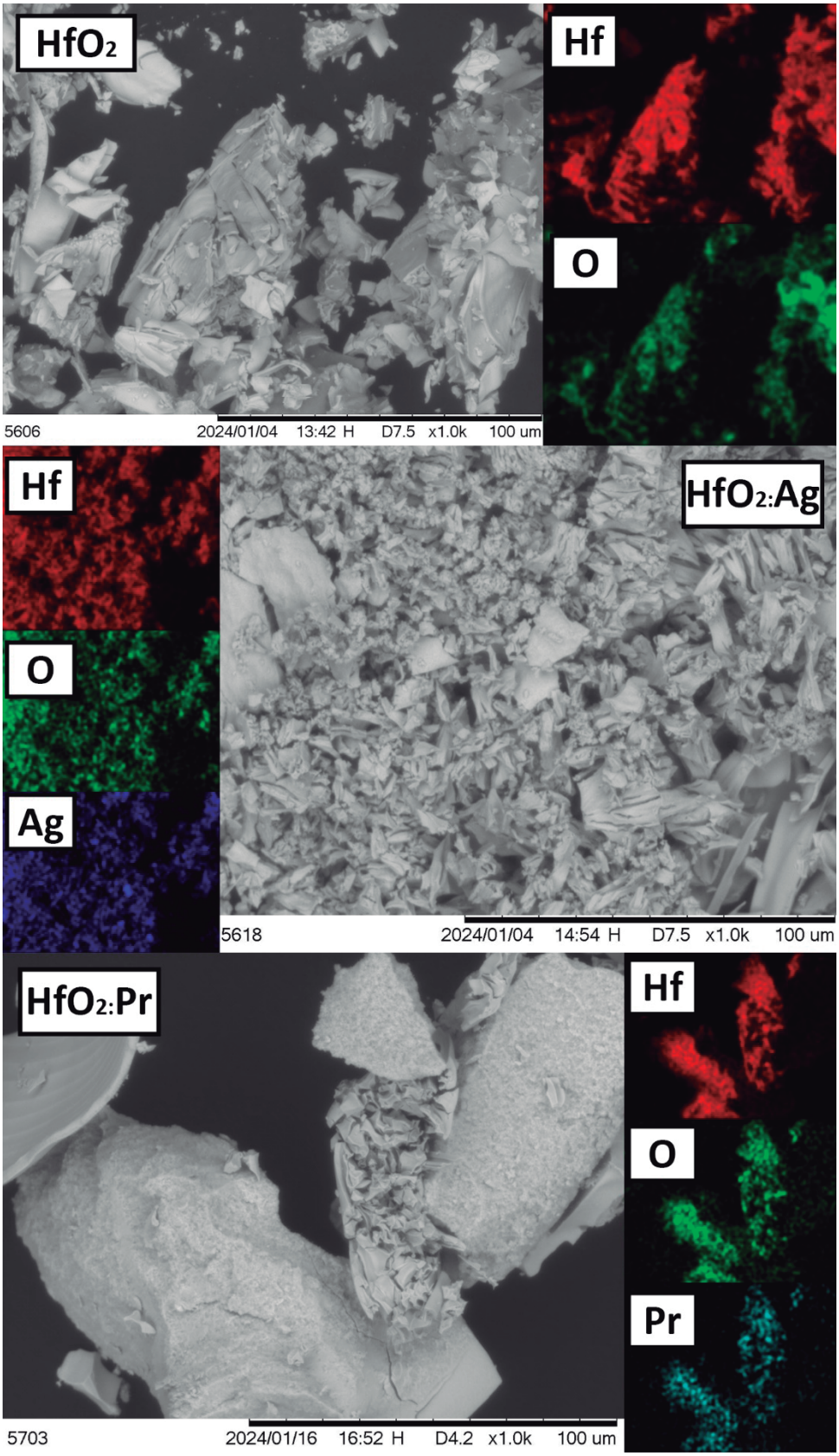

Source: Author's Construction.

Figures 3 and 4 show that all ZrO_2 and HfO_2 samples had agglomerated particles with varying shapes and with size in the order of micrometers, with a tendency to form rough edges. With calcination being a part of the synthesis route, these characteristics are corroborated by previous works (HORTI *et al.*, 2020; SHAH; RATHER, 2021). The presence of more than one phase, as indicated by the XRD results, such as AgCl in the ZrO_2:Ag sample, did not produce any SEM visible characteristics in Figure 3.

The EDS characterization demonstrated a uniform distribution of the elements throughout each sample, with no relevant difference in homogeneity between zirconium, oxygen and its dopants or hafnium, oxygen and its dopants. This is frequently presented as one of the advantages of this synthesis route, which leads to a polymerization process and a good dispersion of the metal ions (GOLYEVA *et al.*, 2020). The multiphasic ZrO_2:Ag and HfO_2 also presented a uniform elemental distribution. This is another indication, along with XRD results, that the formed AgCl was stable and the formation of Ag_2O wasn't favored even at the calcination temperature of 500 ºC, which was also observed in previous studies (SIDDIQUI *et al.*, 2013).

DYNAMIC LIGHT SCATTERING

The dynamic light scattering measurements for hydrodynamic diameter and the polydispersity of each sample suspension can be seen in Table 2:

Table 2 - Hydrodynamic diameter for each dispersed sample obtained using Dynamic Light Scattering.

Sample dispersion	Hydrodynamic diameter (nm)	Polydispersity (%)
ZrO_2 (t)	2686 ± 465	11.9
ZrO_2:Ag (m/t)	3411 ± 723	19.9
ZrO_2:Pr (c)	2753 ± 590	21.6
HfO_2 (m/c)	8486 ± 582	30.2
HfO_2:Ag (m)	972 ± 400	27.7
HfO_2:Pr (c)	2894 ± 1137	23.6

Source: Author's Construction.

It is possible to infer from the data in Table 2 that the agglomeration observed in the previous SEM images occurred for all samples, given that their hydrodynamic diameter reached the order of a few micrometers, with the exception of HfO_2:Ag, with 972 nm. This phenomenon is to be expected for these oxides, since all of them underwent calcination at 500 ºC or above, providing energy through heat, which favors sintering and agglomeration of smaller particles (KLEIN *et al.*, 2023). Additionally, the process of suspending the particles in water may itself result in larger agglomerates (SHAH; RATHER, 2021). All samples showed high values for their polydispersity, with the smallest being pure ZrO_2, with 11.9%. This indicates that the particles not only agglomerated, but this

agglomeration happened in an irregular manner, with a relevant difference in particle size (VOSS *et al.*, 2020). The reduction in the hydrodynamic diameter of HfO_2 and ZrO_2 particles doped with Ag and Pr can be attributed to changes in surface energy and the crystalline structure resulting from doping (SATO *et al.*, 2014).

Furthermore, no surfactant was used at any moment, especially due to the synthesis route requiring calcination. Surfactants such as oleic acid have been used in similar works to induce better homogeneity, smaller particle size and even to reduce their toxicity, but its use depends heavily on the chosen synthesis method (VASILAKAKI; NTALLIS; TROHIDOU, 2023).

DYE DEGRADATION

The results obtained from the degradation assays of crystal violet dye can be seen in Table 3. The results indicate the degradation percentages for various samples, including the blank, tetragonal ZrO_2, a mixture of ZrO_2:Ag in both monoclinic and tetragonal phases, ZrO_2:Pr in the cubic phase, as well as monoclinic and tetragonal HfO_2. Additionally, it includes HfO_2 with Ag in the monoclinic phase, and Hf with Pr in the cubic phase.

Table 3 - Percentage of crystal violet dye degradation for ZrO_2 and HfO_2 samples doped with Ag and Pr in tetragonal, monoclinic and cubic forms.

Sample	Degradation (%)
Blank	15 ± 3
ZrO_2 (t)	24 ± 4
ZrO_2:Ag (m/t)	66 ± 3
ZrO_2:Pr (c)	19 ± 4
HfO_2 (m/c)	71 ± 5
HfO_2:Ag (m)	37 ± 11
HfO_2:Pr (c)	37 ± 5

Legend:
t = tetragonal
c = cubic
m = monoclinic
m/t = mixture of monoclinic and tetragonal
m/c = mixture of monoclinic and cubic

Source: Author's Construction.

When analyzing the blank sample, containing only the dye, it exhibited the lowest degradation rate, as expected. However, for the ZrO_2 stabilized in the tetragonal form, there is a higher degradation rate compared to the blank. Nonetheless, it remains low, given that the material only exists in one phase, and therefore, does not demonstrate significant photocatalytic effects. Conversely, the ZrO_2:Ag with various phases exhibited the second highest degradation rate, potentially attributable to the microstructure's synergistic effect of the metal oxide along with the silver chloride. Additionally,

the presence of different phases further enhances the photocatalytic performance (BAKARDJIEVA *et al*., 2005; NARAGINTI *et al*., 2019).

The ZrO_2 stabilized with Pr in the cubic form exhibited the lowest degradation rate among the various oxides. This variance could be linked to the differing oxidation states of these two elements, namely Zr^{4+} and $Pr^{3+.}$ These ions, with varying oxidation states, can induce distortions in the material's crystal structure, potentially leading to the generation of defects. Consequently, this may decrease the photocatalytic activity of the material, especially considering it only presents one phase (LIANG *et al*., 2009).

The sample with HfO_2 stabilized in the monoclinic and cubic phases exhibited the highest degradation rate among all samples. This outcome is directly linked to the presence of distinct phases in the material, each possessing different surface properties. Consequently, the coexistence of these two phases can substantially enhance the diversity of catalytic active sites for dye degradation, thereby boosting photocatalytic activity. Additionally, this presence can alter the material's band gap, further influencing its performance (BAKARDJIEVA *et al*., 2005; PAUL; CHOUDHURY, 2014).

For the sample of HfO_2:Ag stabilized in the monoclinic phase, a decrease in the dye degradation rate is observed compared to HfO_2 in different phases. The presence of only one phase may have contributed to reducing the synergistic effect between HfO_2 and silver, as samples with mixed phases demonstrate a considerable increase in their photocatalytic activity. Similarly, the sample of HfO_2:Pr stabilized in the cubic phase showed a degradation percentage very similar to that of HfO_2 doped with silver. Thus, it is observed that despite changing the chemical element and the stabilized phase, the degradation percentage did not show a relevant difference. Therefore, the mixture of phases is extremely important to achieve good dye degradation results (BAKARDJIEVA *et al*., 2005; KAKO; YE, 2010).

CONCLUSIONS

The results indicated that the presence of multiple phases in materials such as HfO_2 and ZrO_2 significantly increases the efficiency in dye degradation, suggesting that the coexistence of different phases provides a greater diversity of active catalytic sites. On the other hand, materials with a single phase, such as ZrO_2 and HfO_2 in cubic and monoclinic phases, respectively, showed lower degradation rates, confirming the importance of phase mixture for better results in dye removal. The characterization of the samples revealed the presence of agglomerated particles with uniform distribution of elements, and hydrodynamic diameter measurements indicated a tendency for agglomeration after calcination.

ACKNOWLEDGEMENTS

This study was financed in part by the Coordenação de Aperfeiçoamento de Pessoal de Nível Superior - Brasil (CAPES) - Finance Code 001.

REFERENCES

ARDILA-LEAL, L. D. *et al.* A Brief History of Colour, the Environmental Impact of Synthetic Dyes and Removal by Using Laccases. **Molecules**, v. 26, n. 13, p. 3813, jan. 2021.

BAKARDJIEVA, S. *et al.* Photoactivity of anatase-rutile TiO_2 nanocrystalline mixtures obtained by heat treatment of homogeneously precipitated anatase. **Applied Catalysis B: Environmental**, v. 58, n. 3, p. 193-202, 28 jun. 2005.

BALARAM, V. Rare earth elements: A review of applications, occurrence, exploration, analysis, recycling, and environmental impact. **Geoscience Frontiers**, v. 10, n. 4, p. 1285-1303, 1 jul. 2019.

CARRIELLO, G. M. *et al.* Investigation of Hafnium(IV) Incorporation in Polyurethanes: Structural and Mechanical Properties. **Materials Research**, v. 27, p. e20240132, 6 set. 2024.

DUDEK, M. *et al.* Luminescent properties of praseodymium doped Y_2O_3 and $LaAlO_3$ nanocrystallites and polymer composites. **Journal of Rare Earths**, v. 29, n. 12, p. 1123-1129, 1 dez. 2011.

FAIZAN, S.; BAKHTAWARA; ALI SHAH, L. Facile fabrication of hydrogels for removal of crystal violet from wastewater. **International Journal of Environmental Science and Technology**, v. 19, n. 6, p. 4815-4826, 1 jun. 2022.

GIONCO, C. *et al.* Rare earth oxides in zirconium dioxide: How to turn a wide band gap metal oxide into a visible light active photocatalyst. **Journal of Energy Chemistry**, v. 26, n. 2, p. 270-276, 1 mar. 2017.

GOLYEVA, E. V. *et al.* Nd^{3+} concentration effect on luminescent properties of MgAl2O4 nanopowders synthesized by modified Pechini method. **Journal of Solid State Chemistry**, v. 289, p. 121486, 1 set. 2020.

HARGREAVES, J. S. J. Some considerations related to the use of the Scherrer equation in powder X-ray diffraction as applied to heterogeneous catalysts. **Catalysis, Structure & Reactivity**, v. 2, n. 1-4, p. 33-37, 1 out. 2016.

HORTI, N. C. *et al.* Structural and optical properties of zirconium oxide (ZrO_2) nanoparticles: effect of calcination temperature. **Nano Express**, v. 1, n. 1, p. 010022, abr. 2020.

HU, X. *et al.* Effects of zirconia crystal phases on the catalytic decomposition of N_2O over Co_3O_4/ZrO_2 catalysts. **Applied Surface Science**, v. 514, p. 145892, 1 jun. 2020.

KAKO, T.; YE, J. Synergistic effect of different phase on the photocatalytic activity of visible light sensitive silver antimonates. **Journal of Molecular Catalysis A: Chemical**, v. 320, n. 1, p. 79-84, 1 abr. 2010.

KHOSLA, R. *et al.* Cooling for sustainable development. **Nature Sustainability**, v. 4, n. 3, p. 201-208, mar. 2021.

KLEIN, J. *et al.* Dispersible SnO_2:Sb and TiO_2 Nanocrystals After Calcination at High Temperature. **Small**, v. 19, n. 10, p. 2207674, 2023.

KOCYIGIT, A. *et al.* Improving photocatalytic efficiency: Harnessing the importance of Ag@HfO_2 core-shell nanostructures. **Journal of Physics and Chemistry of Solids**, v. 191, p. 112033, 1 ago. 2024.

KUMARI, H. *et al.* A Review on Photocatalysis Used For Wastewater Treatment: Dye Degradation. **Water, Air, & Soil Pollution**, v. 234, n. 6, p. 349, 26 maio 2023.

LAUDADIO, E. *et al.* Phase Properties of Different HfO_2 Polymorphs: A DFT-Based Study. **Crystals**, v. 12, n. 1, p. 90, jan. 2022.

LAURIA, A. *et al.* Multifunctional Role of Rare Earth Doping in Optical Materials: Nonaqueous Sol-Gel Synthesis of Stabilized Cubic HfO_2 Luminescent Nanoparticles. **ACS Nano**, v. 7, n. 8, p. 7041-7052, 27 ago. 2013.

LI, J. *et al.* Electronic structures and optical properties of monoclinic ZrO_2 studied by first-principles local density approximation + U approach. **Journal of Advanced Ceramics**, v. 6, n. 1, p. 43-49, 1 mar. 2017.

LIANG, C. *et al.* The effect of Praseodymium on the adsorption and photocatalytic degradation of azo dye in aqueous Pr^{3+}-TiO^2 suspension. **Chemical Engineering Journal**, v. 147, n. 2, p. 219-225, 15 abr. 2009.

LIU, H. *et al.* Structural and ferroelectric properties of Pr doped HfO_2 thin films fabricated by chemical solution method. **Journal of Materials Science: Materials in Electronics**, v. 30, n. 6, p. 5771-5779, mar. 2019.

LU, F. *et al.* Phase Transformation of Nanosized ZrO_2 upon Thermal Annealing and Intense Radiation. **The Journal of Physical Chemistry C**, v. 115, n. 15, p. 7193-7201, 21 abr. 2011.

MAHAM, M.; NASROLLAHZADEH, M.; MOHAMMAD SAJADI, S. Facile synthesis of Ag/ZrO_2 nanocomposite as a recyclable catalyst for the treatment of environmental pollutants. **Composites Part B: Engineering**, v. 185, p. 107783, 15 mar. 2020.

MANI, S.; BHARAGAVA, R. N. Exposure to Crystal Violet, Its Toxic, Genotoxic and Carcinogenic Effects on Environment and Its Degradation and Detoxification for Environmental Safety. Em: DE VOOGT, W. P. (Ed.). **Reviews of Environmental Contamination and Toxicology Volume 237**. Cham: Springer International Publishing, 2016. p. 71-104.

NARAGINTI, S. *et al.* Visible light degradation of macrolide antibiotic azithromycin by novel ZrO_2/$Ag@TiO_2$ nanorod composite: Transformation pathways and toxicity evaluation. **Process Safety and Environmental Protection**, v. 125, p. 39-49, 1 maio 2019.

NERIS, A. M. *et al.* Undoped tetragonal ZrO_2 obtained by the Pechini method: thermal evaluation of tetragonal-monoclinic phase transition and application as catalyst for biodiesel synthesis. **Journal of Thermal Analysis and Calorimetry**, v. 143, n. 5, p. 3307-3316, 2020.

ONDRAČKA, P. *et al.* Accurate prediction of band gaps and optical properties of HfO_2. **Journal of Physics D: Applied Physics**, v. 49, n. 39, p. 395301, set. 2016.

PAUL, S.; CHOUDHURY, A. Investigation of the optical property and photocatalytic activity of mixed phase nanocrystalline titania. **Applied Nanoscience**, v. 4, n. 7, p. 839-847, 1 out. 2014.

PAVONI, E. *et al.* The Effect of Y Doping on Monoclinic, Orthorhombic, and Cubic Polymorphs of HfO_2: A First Principles Study. **Nanomaterials**, v. 12, n. 23, p. 4324, jan. 2022.

RAMOS-BRITO, F. *et al.* Preparation and characterization of photoluminescent praseodymium-doped ZrO_2 nanostructured powders. **Journal of Physics D: Applied Physics**, v. 37, n. 5, p. L13, fev. 2004.

RAMOS-GONZÁLEZ, R. *et al.* Study of Hafnium (IV) Oxide Nanoparticles Synthesized by Polymerized Complex and Polymer Precursor Derived Sol-Gel Methods. **Materials Science Forum**, v. 644, p. 75-78, 2010.

SAAD, A. A.; MARTINEZ, C.; TRICE, R. W. Ablation performance of rare earth oxide (REO)-stabilized tetragonal and cubic zirconia coatings as a thermal protection system (TPS) for carbon/carbon composites. **Journal of the European Ceramic Society**, v. 43, n. 14, p. 6449-6460, 1 nov. 2023.

SALAVATI-NIASARI, M.; DADKHAH, M.; DAVAR, F. Pure cubic ZrO_2 nanoparticles by thermolysis of a new precursor. **Polyhedron**, v. 28, n. 14, p. 3005-3009, 23 set. 2009.

SATO, K. *et al.* Surface Capping-Assisted Hydrothermal Growth of Gadolinium-Doped CeO_2 Nanocrystals Dispersible in Aqueous Solutions. **Langmuir**, v. 30, n. 40, p. 12049-12056, 14 out. 2014.

SHAH, A. H.; RATHER, M. A. Effect of calcination temperature on the crystallite size, particle size and zeta potential of TiO_2 nanoparticles synthesized via polyol-mediated method. **Materials Today: Proceedings**, International Conference on Materials, Processing & Characterization. v. 44, p. 482-488, 1 jan. 2021.

SHINDHAL, T. *et al.* A critical review on advances in the practices and perspectives for the treatment of dye industry wastewater. **Bioengineered**, v. 12, n. 1, p. 70-87, 1 jan. 2021.

SIDDIQUI, M. R. H. *et al.* Synthesis and Characterization of Silver Oxide and Silver Chloride Nanoparticles with High Thermal Stability. **Asian Journal of Chemistry**, v. 25, n. 6, p. 3405-3409, 2013.

SINGH, A.; TOMAR, R.; SINGH, N. B. Efficient removal of crystal violet dye from water using zinc ferrite-polyaniline nanocomposites. **Environmental Monitoring and Assessment**, v. 196, n. 6, p. 569, 22 maio 2024.

VASILAKAKI, M.; NTALLIS, N.; TROHIDOU, K. N. Tuning the magnetic properties of oleic-acid-coated cobalt ferrite nanoparticles by varying the surfactant coverage. **Journal of Physics and Chemistry of Solids**, v. 180, p. 111424, 1 set. 2023.

VAZ, F. A. S. *et al.* Construção de câmara de luz ultravioleta para fotopolimerização de fases estacionárias monolíticas. **Química Nova**, v. 31, p. 2156-2158, 2008.

VOSS, L. *et al.* The presence of iron oxide nanoparticles in the food pigment E172. **Food Chemistry**, v. 327, p. 127000, 15 out. 2020.

ZANDIEHNADEM, F.; MURRAY, R. A.; CHING, W. Y. Electronic structures of three phases of zirconium oxide. **Physica B+C**, v. 150, n. 1, p. 19-24, 1 maio 1988.